

## The determination of the influence of heat treatment on the martensitic transformation in Cu–Zn–Al–Mn shape-memory alloy by calorimetry and acoustic emission techniques

F.J. Gil <sup>a</sup> and J.M. Guilemany <sup>b</sup>

<sup>a</sup> *Dept. Ciencia de los Materiales e Ingeniería Metalúrgica, E.T.S. Ingenieros Industriales de Barcelona, Universidad Politécnica de Catalunya, Avda, Diagonal 647, 08028-Barcelona (Spain)*

<sup>b</sup> *Metalurgia Física-Ciencia de Materiales, Facultad de Química, Universidad de Barcelona, c/Martí i Franqués 1, 08028-Barcelona (Spain)*

(Received 22 October 1991)

### Abstract

The influence of two different heat treatments, both carried out at 850°C for a variable testing time with subsequent air cooling or water quenching at room temperature, on the specific temperatures, heat, entropy, chemical enthalpy, elastic contribution and friction work associated with the thermoelastic martensitic transformation in Cu–Zn–Al–Mn shape-memory alloy, was determined. A different number of cycles was performed for each heat treatment, and the changes in the values of these properties were studied.

### INTRODUCTION

The influence of heat treatment on the martensitic transformation in shape-memory alloys has been reported by various authors [1–3]. For copper-based alloys, the work of Rapacioli et al. [1] on Cu–Zn–Al alloys is of particular interest; in the heat treatments carried out in their research, the sample was kept at 850°C and subsequently water quenched at room temperature or aircooled. Their conclusions can be summarized as follows. Quenched material produces a transformation which starts progressively, whereas slow cooling brings about a burst type of transformation. In the air-cooled sample, there is a delay in nucleation but once started, rapid growth follows until total transformation is achieved.

Although the differences in transformation temperatures are very slight, an attempt to explain this behaviour has been made based on the existing differences in the  $\beta$ -matrix, wherein the quenched material shows a greater

---

*Correspondence to:* J.M. Guilemany, Metalurgia Física-Ciencia de Materiales, Facultad de Química, Universidad de Barcelona, c/Martí i Franqués 1, 08028-Barcelona, Spain.

number of vacancies and less  $L_2$  and  $DO_3$  domains than other air-cooled sample [4,5].

The present paper reports the study of the influence of heat treatment on a new quaternary shape-memory alloy, Cu–Zn–Al–Mn. The addition of manganese brings about a considerable improvement in the mechanical properties and an increase in the range of transformation temperatures [6].

In these alloys, 18R orthorhombic and 2H hexagonal martensites with electron-to-atom ratios above 1.43 coexist [7]. This is demonstrated by X-ray diffraction [8], calorimetric [9,10] and TEM studies [11].

## EXPERIMENTAL PROCEDURE

This study was carried out on two polycrystalline samples of the same chemical composition (19.28% Al, 6.09% Zn, 3.44% Mn, in atomic percentage) in their as-cast state. The samples were cut into cylinders 5 mm in diameter and 3 mm high, with an approximate weight of 400 mg. One of the samples was submitted to five successive heating cycles at 850°C for 1 min and air-cooled (TT1). Another of the samples underwent 10 successive heating cycles at 850°C for 1 min and water quenching at 25°C (TT3). In each of the heat treatment cycles carried out, calorimetric thermograms were obtained as well as acoustic emission registers.

The experimental measurements were carried out 24 h after heat treatment. In this work, a multi-cell flow calorimeter was used, measuring the differential signals ( $\Delta T$ ) using Melcor FC06-32-06L thermobatteries made up of 32 thermocouples, and using a temperature range from  $-150$  to  $100^\circ\text{C}$ . The temperature was measured by a Pt-100 standard sond. All the signals were digitized by a multichannel analyser and stored on a computer [12,13]. The sensitivity of the differential signal detectors was  $400 \text{ mV W}^{-1}$  at room temperature. The uncertainty was less than 5% in the enthalpy and entropy variants and  $\pm 0.5 \text{ K}$  in the temperatures. The heating-cooling rate was  $1^\circ\text{C min}^{-1}$  [12,13].

The acoustic emission generated during transformations can be detected and converted into electrical signals which can be recorded. In this work, the temperatures and transformation heats were determined simultaneously by the above-mentioned calorimetric system and by acoustic emission.

The piezoelectric detector signal was amplified 51 dB on the 50–2 MHz band and digitized by a frequency counter. The sample acquires data every 3.5 s. The diagrams resulting from the acoustic emission detection show a greater irregularity than the calorimetric diagrams. The base lines are composed of small peaks due to background noise. When transformation is produced, the acoustic signal leaves the base line and forms large peaks until the signal returns to the base line. The particular transformation temperatures are indicated in the same way as the calorimetric tempera-

tures, i.e. those temperatures at which the acoustic signal begins to increase, leaving the base line and when it returns to the base line [12].

The thermodynamic study of this quaternary alloy was performed according to the recent thermodynamic model proposed by Ortín and Planes [14] for the thermoelastic martensitic transformation, which provides the possibility of its evaluation by means of calorimetric data. This model may be applied in the TT1 heat treatment because the coexistence of 2H and 18R martensite is small and because there is only a slight irreversible entropy effect.

## EXPERIMENTAL RESULTS AND DISCUSSION

The transformation temperatures  $M_s$ ,  $M_f$ ,  $A_s$  and  $A_f$  were measured after each heat treatment from the calorimetric and acoustic emission registers obtained. This can be seen in Fig. 1 in the heating and cooling cycles of the first treatment for sample TT3, and in Fig. 2 for TT1.

The transformation temperatures are shown in Tables 1 and 2 for TT3 and TT1 heat treatments, respectively, as measured by calorimetry; Tables 3 and 4 show those measured by acoustic emission detection.

It can be seen that  $M_s$  increases with the number of cycles in both heat treatments studied; this means that the transformation becomes easier to carry out. While the material is being cycled, dislocations are created as a result of residual strain in the structure during transformation; these dislocations are formed in the  $\beta$ -phase–martensite interphases [15,16] and remain in the matrix when the material retransforms. These dislocations formed in the cycling process bring about martensite stabilization, with the result that part of it no longer transforms and that the retained martensite favours the nucleation of new plates. This explains the observed increase in the  $M_s$  temperature.

Another reason for this increase in  $M_s$  is the fact that heat treatments stimulate both linear defects and vacancies. These defects include internal stress in the structure which help the martensitic transformation as well as providing a large number of potential places for martensitic nucleation.

The martensite stabilization can be noted by the fact that the  $A_s$  temperatures increase with the number of cycles, as do the differences between the  $M_f$  and  $A_f$  temperatures. This stabilization is greater in Cu–Zn–Al–Mn alloys than in copper-based Cu–Zn–Al [17], Cu–Al–Ni [6] or Cu–Al–Mn [18] alloys, owing to two important factors:

1. In the Cu–Zn–Al–Mn alloys, over a wide range of electron-to-atom ratios, two types of martensite coexist: orthorhombic, 18R, and hexagonal, 2H. These two structures do not have self-accommodating plates and therefore mechanical anchorages are formed, impeding retransformation.
2. The high density of vacancies produced in these treatments brings about a slight increase in the  $A_s$  transformation temperatures. This has

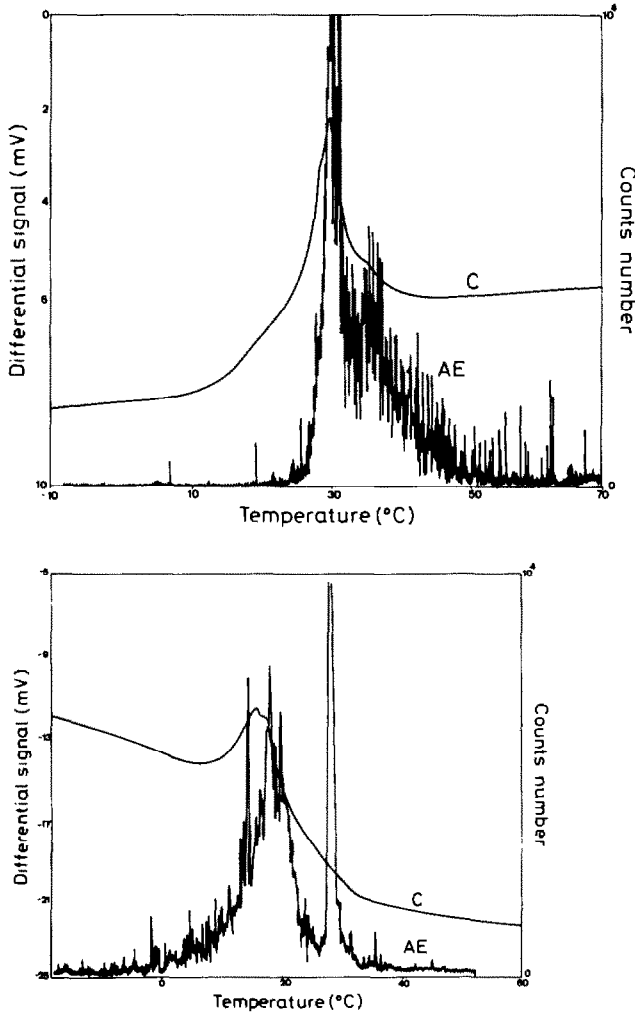


Fig. 1. Calorimetric (differential signal) and acoustic emission (in counts number) registers in the heating (upper) and cooling (lower) cycles of the first heat treatment TT3.

been studied by Zhao et al. [11] by means of positron absorptions (PAS). These authors affirm that the vacancies obstruct interphase movement of the martensitic plates. Furthermore, the excess of vacancies favours the start of martensite ageing by factors of 100–500. The precipitates formed during ageing prevent total retransformation.

If the Ms results are compared for both heat treatments, it can be seen that the temperatures at the start of the martensitic transformation are higher in TT1 than in TT3. The  $\beta$ -phase is disordered at high temperatures but undergoes an ordering when it is stabilized at low temperatures [ $DO_3$  or  $L_2$  order structures). The air-cooled sample favours the coexistence of two  $\beta$ -orders, which leads to the formation of two types of martensite (18R

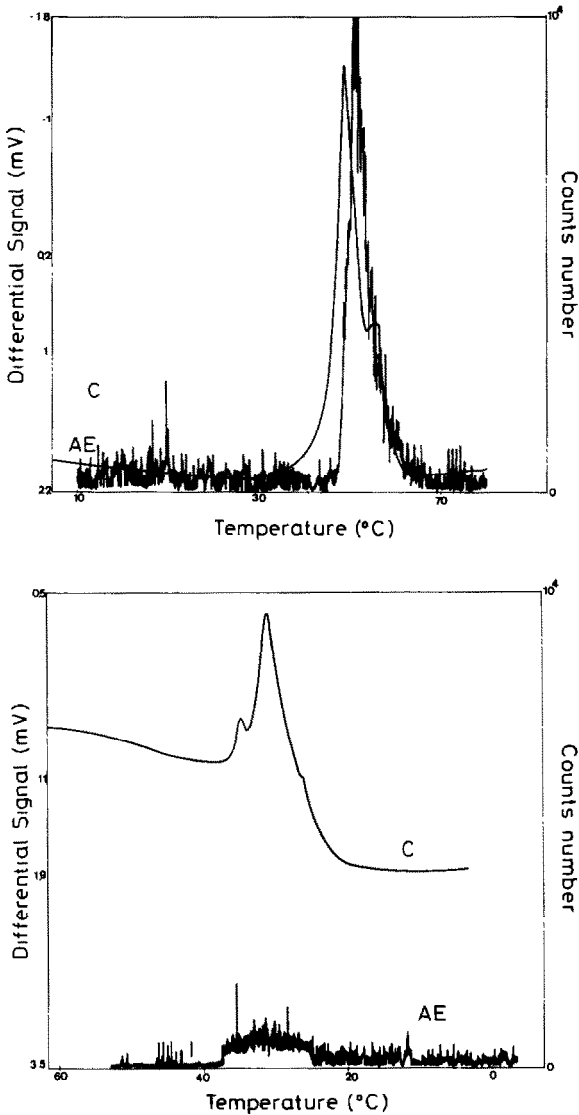


Fig. 2. Calorimetric (differential signal) and acoustic emission (in counts number) registers in the heating (upper) and cooling (lower) cycles of the first heat treatment TT1.

and 2H). This can be seen in Fig. 2 in the heating and cooling cycles of the first heat treatment TT1, where the calorimetric registers have two peaks corresponding to the two types of martensite. The martensite transformation of shape-memory alloys is generally characterized by a unique self-accommodation among various variants; the coexistence of different types of martensites should result in complex mixtures of various interfaces with different substructures between martensite variants and groups, so that the self-accommodation of the various martensite variants would be incom-

TABLE 1

Transformation temperatures (°C) for TT3 heat treatment, obtained by calorimetry

Cycle	Ms	Mf	As	Af
1	22	2	10	42
2	26	-2	12	45
3	28	-3	13	45
4	30	9	14	48
5	30	8	17	48
6	31	10	20	49
7	33	7	20	49
8	33	10	20	52
9	33	10	20	53
10	33	11	21	55

TABLE 2

Transformation temperatures (°C) for TT1 heat treatment, obtained by calorimetry

Cycle	Ms	Mf	As	Af
1	39	21	33	61
2	40	21	37	62
3	42	22	49	64
4	42	24	49	64
5	42	24	49	65

plete. This would cause more distorted transition regions, which favours the start of martensitic transformation. Therefore, the start of martensitic transformation will be favoured more in TT1 heat treatment rather than TT3.

If comparison studies are made of transformation temperatures obtained simultaneously by calorimetry and acoustic emission, it can be seen that:

TABLE 3

Transformation temperatures (°C) for TT3 heat treatment, obtained by acoustic emission

Cycle	Ms	Mf	As	Af
1	32	-12	16	65
2	34	-11	18	66
3	36	-6	19	66
4	36	-7	21	70
5	37	4	23	65
6	44	6	23	66
7	44	7	24	70
8	44	8	26	74
9	44	8	26	77
10	44	8	27	77

TABLE 4

Transformation temperatures (°C) for TT1 heat treatment, obtained by acoustic emission

Cycle	Ms	Mf	As	Af
1	43	29	34	68
2	43	29	39	64
3	44	30	50	65
4	44	31	50	69
5	44	31	50	69

values of Ms determined by acoustic emission are higher than those of the calorimetric signal; the acoustic emission signal is still present above the Af calorimetric temperatures.

This phenomenon also takes place in other shape-memory alloys which have been studied in situ by scanning electron microscopy [19]. This shows that the occurrence of a  $\beta$ -phase acoustic emission before the Ms calorimetric temperature corresponds to martensitic plates which are apparent at least on the surface. These plates later disappear during the overall transformation to be replaced by others that may be better oriented or may have local distribution of the provoked stress in the transformation itself. A  $\beta$ -phase acoustic emission above the Af calorimetric temperature corresponds to the new appearance of similar plates after the martensite  $\rightarrow$   $\beta$  retransformation, as seen microscopically. These plates always have the same orientation as those which were detected before the calorimetric Ms temperature. These plates finally disappear if the sample is heated above the calorimetric Af temperature.

From the acoustic emission registers in Figs. 1 and 2,  $\beta \rightarrow$  martensite and martensite  $\rightarrow$   $\beta$  asymmetry can be seen in both heat treatments. This means that the acoustic emission generated in the inverse transformation is more intense than that generated in the direct transformation. The fact that it is more intense than in other alloys, such as Cu–Zn–Al, is because in the  $\beta \rightarrow$  martensite transformation, elastic-type energies are stored in the structure which can be released as acoustic emission on retransformation. Another cause of this difference can be attributed to the increase in acoustic emission when there is friction work between the martensitic plates or between the matrix phase and the martensite [20,21]. In Cu–Zn–Al–Mn alloys, these effects are greater in the reverse transformation owing to the stabilization of non-self-accommodating martensitic plates and, in addition, to the anchorages present with both linear and vacancy defects.

Heat  $Q$ , entropy  $\Delta S$  and chemical enthalpy  $\Delta H_{\text{chem}}$  transformation values are shown in Table 5 for TT3 and in Table 6 for TT1. The thermodynamic variants of both heat treatments are very similar because they depend only on the initial and final states, not on the heat treatment which is being carried out. The results obtained for the heat, entropy and

TABLE 5

Heat, entropy and chemical enthalpy values for each TT3 heat treatment

Cycle	$Q$ ( $\text{J g}^{-1}$ )	$\Delta S$ ( $\text{J g}^{-1} \text{K}^{-1}$ )	$\Delta H_{\text{chem}}$ ( $\text{J g}^{-1}$ )
1	6.9	2.31	7.04
2	6.9	2.30	7.09
3	6.1	2.04	6.30
4	4.5	1.50	4.63
5	5.0	1.65	5.16
6	5.4	1.77	5.55
7	5.1	1.30	5.31
8	4.1	1.36	4.30
9	4.9	1.64	5.20
10	4.5	1.50	4.75

TABLE 6

Heat, entropy and chemical enthalpy values for each TT1 heat treatment

Cycle	$Q$ ( $\text{J g}^{-1}$ )	$\Delta S$ ( $\text{J g}^{-1} \text{K}^{-1}$ )	$\Delta H_{\text{chem}}$ ( $\text{J g}^{-1}$ )
1	6.9	2.20	7.10
2	6.5	2.10	6.73
3	6.4	2.03	6.64
4	6.2	1.98	6.45
5	6.2	1.98	6.45

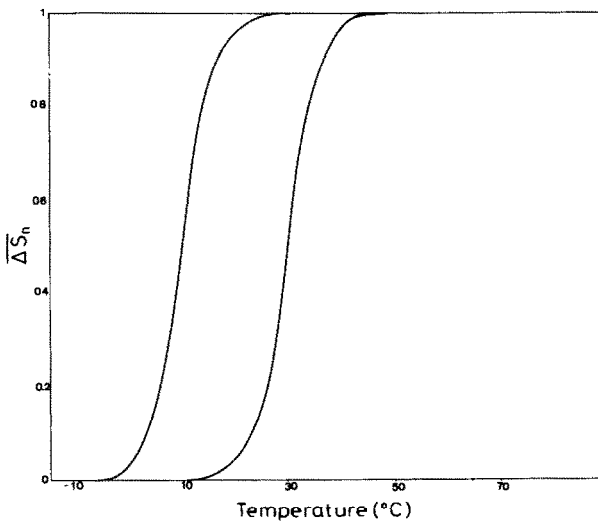


Fig. 3. Hysteresis cycle of TT3 sample.



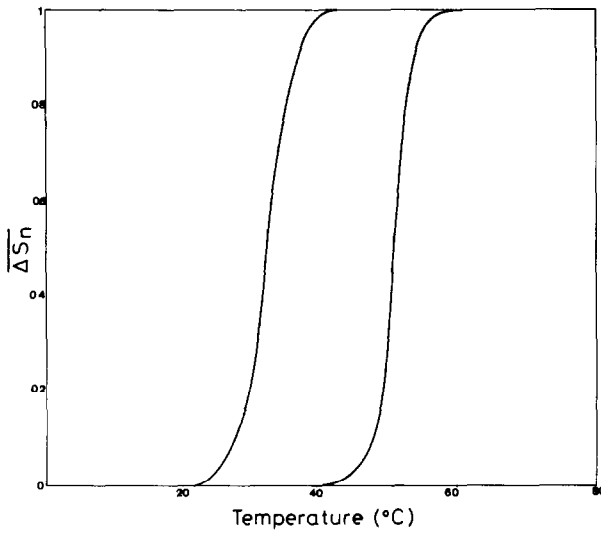


Fig. 4. Hysteresis cycle of TT1 sample.

TABLE 7

Elastic and friction energies for each TT3 heat treatment

Cycle	$\Delta H_{el}$ ( $J g^{-1}$ )	$E_{fr}$ ( $J g^{-1}$ )
1	0.14	0.25
2	0.14	0.28
3	0.16	0.26
4	0.16	0.27
5	0.17	0.29
6	0.19	0.30
7	0.19	0.32
8	0.20	0.32
9	0.21	0.32
10	0.21	0.32

TABLE 8

Elastic and friction energies for each TT1 heat treatment

Cycle	$\Delta H_{el}$ ( $J g^{-1}$ )	$E_{fr}$ ( $J g^{-1}$ )
1	0.20	0.37
2	0.21	0.37
3	0.21	0.38
4	0.23	0.40
5	0.23	0.40

chemical enthalpy values show a decrease with increasing number of cycles, being greater in direct than in indirect transformation, in all cases. This can be explained by the fact that some martensitic plates do not retransform to  $\beta$ -phase, owing to stabilization; therefore, total retransformation will not occur.

The friction energy is obtained by calculating the area within the hysteresis cycles (normalized entropy versus temperature); a TT3 sample is shown in Fig. 3 and a TT1 sample in Fig. 4. The elastic and friction energy values increase with the number of cycles in the heat treatment studied, see Tables 7 and 8; this can be explained by the fact that the defects grow with successive cycling. These defects obstruct interphase movement, producing the increase in elastic and friction energies. However, from the seventh TT3 treatment and the first TT1 treatment, these values tend to be constant because they do not increase indefinitely.

#### ACKNOWLEDGEMENT

The present research was supported by CICYT project MAT 89-0407-C03-02.

#### REFERENCES

- 1 R. Rapacioli, J.L. Macqueron and G. Guenin, Influencia de la historia térmica sobre la transformación martensítica, *Jornadas de las Transformaciones Termoelásticas*, Univ. Islas Baleares, (1984) 602–610.
- 2 C. Auguet, E. Cesari and L.L. Mañosa, 14 èmes Journées des Equilibres entre Phases, *JEEP*, 1 (1988) 23 Montpellier.
- 3 J. Muntasell, J.L. Tamarit, J.M. Guilemany, F.J. Gil and E. Cesari, *Mater. Res. Bull.*, 23 (1988) 1585–1590.
- 4 R. Rapacioli and M. Ahlers, *Scr. Metall.*, 11 (1979) 1147.
- 5 R. Rapacioli, M. Chandrasekaran and F.C. Lovey, in M.I. Adronson (Ed.), *Proceedings of Solid Transformations*, Oxford, 1981.
- 6 E. Aernordt, J. Van Humbeck, L. Delaey and W. Van Moorlegem, *Proc. 7th Int. Conf. Copper*, Barga, Italy, 1986, p. 8.
- 7 J.M. Guilemany and F.J. Gil, *Mater. Res. Bull.*, 27 (1991) 245.
- 8 J.H. Yang, Z.S. Zhang, L.C. Zhao and T.C. Lei, *Scr. Metall.*, 21, (1987) 259.
- 9 C. Segui, J. Van Humbeck and E. Cesari, *Congreso de la Real Sociedad Española de Física*, Actas del Congreso, ISBN 84-7632-062-0, 1989, pp. 231–232.
- 10 J.M. Guilemany and F.J. Gil, *J. Mater. Lett.*, 10(3) (1990) 145–148.
- 11 L.C. Zhao, J.H. Vang, C.S. Zhang, T.C. Lei, H. Gu and Y.S. He, *Scr. Metall.*, 20 (1986) 29–32.
- 12 J.M. Guilemany and F.J. Gil, *Rev. Metall. CENIM.*, 25(6) (1989) 398–404.
- 13 J.M. Guilemany and F.J. Gil, *Thermochim. Acta*, 161 (1990) 23–27.
- 14 J. Ortin and A. Planes, *Acta Metall.*, 36 (1988) 1873–1888.
- 15 K. Marukava and S. Kaliwava, *Philos. Mag. A*, 55(1) (1975) 85.
- 16 D. Rios Jara, M. Marin, C. Esnort and G. Guenin, *Scr. Metall.*, 19 (1985) 441.
- 17 J.V. Humbeck, J. Jansen, M. Wanban and L. Delaey, *Scr. Metall.*, 18 (1984) 893.

- 18 J.M. Guilemany and F. Peregrin, *J. Mater. Sci.*, 27 (1992) 863–868.
- 19 F.J. Gil, Doctoral Thesis, Universidad de Barcelona, 1989.
- 20 C. Picornell, Doctoral Thesis, Universidad Islas Baleares, 1988.
- 21 C. Segui, Doctoral Thesis, Universidad Islas Baleares, 1988.